

Double exchange and orbital correlations in electron doped manganites

Tulika Maitra^{*1} and A. Taraphder^{*†2}

^{*}Department of Physics & Meteorology and Centre for Theoretical Studies,
Indian Institute of Technology, Kharagpur 721302 India
and

[†]Department of Physics & Astronomy, Michigan State University,
East Lansing, MI 48823-1116

Abstract

A double exchange model for degenerate e_g orbitals with intra- and inter-orbital interactions has been studied for the electron doped manganites $A_{1-x}B_x\text{MnO}_3$ ($x > 0.5$). We show that such a model reproduces the observed phase diagram and orbital ordering in the intermediate bandwidth regime and the Jahn-Teller effect, considered to be crucial for the region $x < 0.5$, does not play a major role in this region. Brink and Khomskii have already pointed this out and stressed the relevance of the anisotropic hopping across the degenerate e_g orbitals in the infinite Hund's coupling limit. From a more realistic calculation with finite Hund's coupling, we show that inclusion of interactions stabilizes the C-phase, the antiferromagnetic metallic A-phase moves closer to $x = 0.5$ while the ferromagnetic phase shrinks. This is in agreement with the recent observations of Kajimoto et. al. and Akimoto et. al.

PACS Nos. 75.30.Et, 75.30.Vn

The perovskite manganites have been at the centre of attention[1, 2] recently as systems like $\text{Pr}_{1-x}\text{Ca}_x\text{MnO}_3$, $\text{La}_{1-x}\text{Ca}_x\text{MnO}_3$, exhibit colossal magnetoresistance (CMR). These two extensively studied systems have relatively low bandwidths. The observation of CMR even in the wider bandwidth materials like $\text{Pr}_{1-x}\text{Sr}_x\text{MnO}_3$ [3] and $\text{Nd}_{1-x}\text{Sr}_x\text{MnO}_3$ for $x \geq 0.5$ [4] have prompted a series of careful experimental work on the magnetic phase diagram of all of these systems particularly in the region $x \geq 0.5$ (the so called *electron doped regime*). This region shows a rich variety of magnetic and orbital ordering and only recently the systematics of the phase diagram with externally controlled bandwidth have begun to emerge[5].

In their study of $\text{Pr}_{1-x}\text{Sr}_x\text{MnO}_3$, Kajimoto et. al.[6] have summarized the nature of magnetic ordering for a series of manganites having different bandwidths (Fig.1 in ref.[6]). They observe that there is no CE phase in many of these systems and the sequence of phases in the electron doped region for moderate to large bandwidth systems follows the order ferromagnetic (F) \rightarrow A-type antiferromagnetic (AFM) \rightarrow C-type AFM and finally to G-type AFM phase. The F phase close to $x = 0.5$ is very narrow and survives for systems

¹email: tulika@phy.iitkgp.ernet.in

²email: arghya@phy.iitkgp.ernet.in, arghya@pa.msu.edu

with bandwidths above $\text{Pr}_{0.5}\text{Sr}_{0.5}\text{MnO}_3$ (e.g., in $(\text{La}_{0.5}\text{Nd}_{0.5})_{1-x}\text{Sr}_x\text{MnO}_3$ there is a small sliver of F metallic phase[5]). A-phase exists in a small region while the C-phase covers the widest region in the phase diagram. The general trend is that with decreasing bandwidth the F-phase reduces, A-phase moves closer to $x = 0.5$ while the C-phase grows. It is also observed that the gradual building of AFM correlations, starting from $x = 0.5$, is preempted by the orbital ordering in the A and C phases[7, 8]. There does not seem to be any convincing evidence in favour of phase separation in this region[6].

In the absence of Jahn-Teller (JT) splitting the two e_g orbitals of Mn ion are degenerate. The doped manganite $\text{R}_{1-x}\text{A}_x\text{MnO}_3$ has $y = 1 - x$ number of electrons in the e_g orbitals and the filling, therefore, is $\frac{y}{4}$. In the foregoing, we restrict ourselves to the region $x \geq 0.5$ i.e., $y \leq 0.5$. At the $x = 1$ end, the band is empty and the physics is governed entirely by the exchange between the t_{2g} electrons in the neighbouring sites. On doping, the kinetic energy of electrons in the e_g levels begin to compete with the AF superexchange (SE) between neighbouring t_{2g} spins via Hund's coupling and this leads to a rich variety of magnetic and orbital structures. A model incorporating this physics has recently been proposed by Brink and Khomskii[9] (hereinafter referred to as BK).

The model BK used for the electron-doped manganites contains three terms

$$H = J_{AF} \sum_{\langle ij \rangle} \mathbf{S}_i \cdot \mathbf{S}_j - J_H \sum_i \mathbf{S}_i \cdot \mathbf{s}_i - \sum_{\langle ij \rangle \sigma, \alpha, \beta} t_{i,j}^{\alpha\beta} c_{i,\alpha,\sigma}^\dagger c_{j,\beta,\sigma} \quad (1)$$

The first term represents the AF exchange between t_{2g} spins, the second term is the Hund's coupling between t_{2g} and e_g spins at each site and the third one provides hopping between the two orbitals[10] (α, β take values 1 and 2 for $d_{x^2-y^2}$ and $d_{3z^2-r^2}$ orbitals, corresponding to the choice $\xi_i = 0$ in Ref.[11]).

The existence of the degenerate e_g orbitals with the asymmetric hopping integrals $t_{ij}^{\alpha\beta}$ makes (1) very different from the usual DE model[1]. BK treated the t_{2g} spins quasi-classically and J_H was set to infinity. Canting in the x-z plane was included through the effective hoppings $t_{xy} = t \cos(\theta_{xy}/2)$ and $t_z = t \cos(\theta_z/2)$. Here θ_{xy} (θ_z) is the angle between nearest neighbour t_{2g} spins in the x-y plane (z-direction). The superexchange energy per state, then, is $E_{SE} = \frac{J_{AF} S_0^2}{2} (2 \cos \theta_{xy} + \cos \theta_z)$. At this level of approximation, the problem reduces to solving the 2×2 matrix equation $||t_{\alpha\beta} - \epsilon \delta_{\alpha\beta}|| = 0$ for a system of spinless fermions and minimizing the total energy with respect to θ_{xy} and θ_z . In the uncanted state, $\theta_{xy} = \theta_z = 0$ implies F phase, $\theta_{xy} = \theta_z = \pi$ G-type, $\theta_{xy} = \pi$ and $\theta_z = 0$ C-type and $\theta_{xy} = 0$ and $\theta_z = \pi$ A-type AFM phases.

Remarkably, the phase diagram obtained by BK based on such simplifying assumptions indeed shows the different magnetic phases seen experimentally in $\text{Nd}_{1-x}\text{Sr}_x\text{MnO}_3$ and $\text{Pr}_{1-x}\text{Sr}_x\text{MnO}_3$ in the region $x > 0.5$ although the G-phase, expected for the nearly empty band (close to $x = 1$) and the F state at $J_{AF} \rightarrow 0$ were, however, not recovered. The limit of infinite Hund's coupling which BK worked with is somewhat unphysical for the manganites considered[12, 13, 14]. In a more realistic treatment Pai[16] considered the limit of finite J_H and succeeded in recovering the G and F phases.

From these results BK argue that the degeneracy of e_g orbitals and the anisotropy of

hopping are crucial and the JT effect not quite as relevant since the number of JT centres is low in the range of doping considered. The effect of disorder, completely ignored in this model, does not seem to play a major role in the magnetic phase diagram[16].

Neither of the treatments of BK and Pai include the interactions present in the system, namely the inter- and intra-orbital Coulomb interactions as well as the intersite Coulomb interaction[12, 13, 17]. Although for low doping the interactions are expected to be ineffective, with increase in doping they tend to localize the carriers and preferentially enhance the orbital ordering. This affects the F-phase and alters the relative stability of A and C phases. It is, therefore, necessary to include them in the Hamiltonian (1) and look for their effects on the phase diagram. A natural extension to the model (1) is then[12]

$$H_{int} = U \sum_{i\alpha} n_{i\alpha\uparrow} n_{i\alpha\downarrow} + U' \sum_{i\sigma\sigma'} n_{i1\sigma} n_{i2\sigma'} \quad (2)$$

Here U and U' represent the intra- and inter-orbital Coulomb interaction strengths. For the systems concerned, we are not looking for the charge ordered states[18] and neglect longer range interactions. We take the interactions U and U' as parameters as in[11, 14] while in reality, these are related through the Racah parameters(see [12] and references therein). We treat the spin system quasi-classically, but unlike BK we work at finite Hund's coupling. In the uncanted states, we assume for the t_{2g} spin $\mathbf{S}_i = \mathbf{S}_0 \exp(i\mathbf{Q}\cdot\mathbf{r}_i)$, where the choice of \mathbf{Q} determines different spin arrangements for the core spins. In the infinite J_H limit, the e_g electron spins would be forced to follow the core spins leading to the freezing of their spin degrees of freedom. A finite value for J_H , however, allows for fluctuations and the spin degrees of freedom, along with anisotropic hopping across the two orbitals, play a crucial role.

Let us first look at the Hamiltonian (1) i.e., set $U = U' = 0$. For t_{2g} spin configurations described above, it reduces to

$$H = \sum_{\mathbf{k}, \alpha, \beta, \sigma} \epsilon_{\mathbf{k}}^{\alpha\beta} c_{\mathbf{k}\alpha\sigma}^\dagger c_{\mathbf{k}\beta\sigma} - J_H S_0 \sum_{\mathbf{k}, \alpha} c_{\mathbf{k}\alpha\uparrow}^\dagger c_{\mathbf{k}+\mathbf{Q}\alpha\uparrow} + J_H S_0 \sum_{\mathbf{k}, \alpha} c_{\mathbf{k}\alpha\downarrow}^\dagger c_{\mathbf{k}+\mathbf{Q}\alpha\downarrow} \quad (3)$$

where we have followed the notation in[10] for $\epsilon_{\mathbf{k}}^{\alpha\beta}$.

We calculate the ground state energy by diagonalization of the above Hamiltonian in a finite momentum grid (numerical results converged by a grid size $64 \times 64 \times 64$) as a function of J_H for a range of values of J_{AF} . The magnetic phase diagram for $J_{AF} S_0^2 = 0.05$ in the $J_H - x$ plane is shown in Fig.1a. The phase diagram in $J_{AF} - x$ plane for $J_H S_0 = 10$ is plotted in Fig.2a. All energies are measured in units of the hopping t . There is no general agreement on the values of the parameters involved[12]. From photoemission and optical studies[12, 13] and LDA analysis[15]) one can glean a range of typical values $0.1eV < t < 0.3eV$, $J_H \simeq 1.5 - 2$ eV and $J_{AF} \simeq 0.03t - 0.1t$ (Maezono et. al.[19] quote a lesser value of $J_{AF} = 0.01t$).

At the $x = 1$ end, with empty e_g orbitals, the only contribution to energy comes from the SE interaction leading to the G-type AFM phase. On doping by electrons the C-phase appears first with orbital ordering (of the d_{z^2} orbitals) along the z-direction. The stability of the A-phase comes from the ordering of $d_{x^2-y^2}$ orbitals in the xy plane. The gain in kinetic

energy due to the planar and one dimensional orbital order, induced by the anisotropic hopping integral, more than offsets the loss of SE energy. The orbital order drives the corresponding magnetic order as well - in the A-phase the spins have planar FM order and AFM order along the z-direction whereas in the C-phase it is reversed. The 3D magnetically ordered F- and G-phases show no orbital ordering. The phase transitions are therefore characterised by the density of states (DOS) reflecting the underlying 1, 2 and 3 dimensional characters of the different phases. The phase diagrams are shown in Figs.1a and 2a, for typical values of the parameters $J_H S_0 = 10$ and $J_{AF} S_0^2 = 0.05$. The sequence of G, C, A and finally the F phase with complete alignment of spins is observed.

In the infinite Hund's coupling limit the "wrong" spin sector of the Hilbert space was projected out by BK. When the system is doped, spin canting is the only channel for delocalization of doped carriers, albeit with a loss in SE energy. At finite J_H , however, the wrong spins are no longer as "costly" and canting is expected to reduce. Canting is included through the choice $\mathbf{S}_i = \mathbf{S}_0(\sin\theta_i, 0, \cos\theta_i)$. The Hund's coupling term in the Hamiltonian becomes $H_{hund} = -J_H S_0 \sum_{i,\alpha} \cos\theta_i (c_{i\alpha\uparrow}^\dagger c_{i\alpha\uparrow} - c_{i\alpha\downarrow}^\dagger c_{i\alpha\downarrow}) - J_H S_0 \sum_{i,\alpha} \sin\theta_i (c_{i\alpha\uparrow}^\dagger c_{i\alpha\downarrow} + c_{i\alpha\downarrow}^\dagger c_{i\alpha\uparrow})$. In this case the different magnetic phases need to be defined at the outset. The convention used by BK to define the magnetic phases are: it is A-type when $\theta_{xy} < \theta_z$ and C-type when $\theta_{xy} > \theta_z$. In the canted G and F phases θ_{xy} and θ_z are close to 180° and 0° respectively, although, it is obvious that the canted G-phase and A-phase are synonymous in a certain region. However, orbital order can be used to delineate the two phases[21].

Proceeding as before, the ground state energy for different θ_{xy} and θ_z is obtained. The qualitative phase diagram is very similar to the uncanted case except for small shifts in the phase boundaries (the shifts are small unless J_H is large) and agrees[23] with Pai[16]. We show in Fig.3 the angle of canting for both θ_z and θ_{xy} deep inside the G-phase at $x = 0.98$. The angles in Fig.3 represent deviation from 180° . There is hardly any canting in θ_z while in θ_{xy} , there is no significant canting for low J_H and it is about 10° only for large J_H . We note that experiments[5, 7] have so far not been able to detect any significant canting in A- and C-phases. Even in the G-phase, certain systems appear to show little canting.

The interactions (both intra- and inter-orbital) are treated in the mean-field (MF) theory and a self-consistent calculation has been performed. Self-consistency is achieved when all the averages $\langle \hat{n}_{i,\sigma,\alpha} \rangle$ and the ground state energy converge to within 0.01%. Figs.1a,b and 2a,b show the modifications in the magnetic phase diagram by the inter-orbital (U') interaction in the $x - J_H$ plane at $J_{AF} S_0^2 = 0.05$ and in the $x - J_{AF}$ plane for $J_H S_0 = 10$. Although we obtained the phase diagram for several values of U' , in Figs.1,2 we only give representative ones for demonstration. On increasing U' , the F-phase starts shrinking fast, the C-phase gains in size while the G-phase remains almost unaltered. This is primarily because of the enhanced orbital ordering in the A- and C-phases driven by the inter-orbital repulsion and the low dimensional nature of the DOS in these phases. As discussed earlier the AFM A and C phases are driven by orbital ordering and in the presence of U' , the one dimensional order leading to the AF instability in the C-phase grows faster. Close to the $x = 1$ end the electron density is very low, there are almost no sites with both the orbitals occupied and U' is therefore ineffective. At the other end, however, the density is higher and

the F phase has preferential occupation of one spin at both the orbitals. Hence this phase is affected drastically by the inter-orbital repulsion.

It is known[11, 12] that at the level of MF theory the intra- orbital repulsion U between opposite spins mimics the effect of J_H . As we are working with quite low densities (actual filling ≤ 0.125), and the relevant J_H values being large, we find almost no observable effect of U on the phase diagram (except for very low J_H where again the changes are small).

In the absence of interactions there is orbital ordering in both A- and C-phases. The presence of U' enhances this ordering. We calculate the orbital densities in both A- and C-phases in the respective ground states and show the results in Fig.4. In the figure, we have plotted actual orbital occupancies (the sum of the occupancies of the two orbitals will be $\frac{1-x}{4}$) for different U' . It is evident from the figure that in the A-phase the $d_{x^2-y^2}$ orbitals are predominantly occupied, while in the C-phase the d_{z^2} orbitals have higher occupancy. As U' increases, the orbital ordering is enhanced. This is shown in Fig.4 for three values of U' in the A and C phases in their respective regions of stability as a function of doping. Note that as x increases (density of electron decreases), the effect of U' on the orbital occupancies becomes less pronounced and the curves for different U' merge as expected. We also show the orbital occupancies as a function of U' in Fig.5 in the regions where A- and C-phases are stable and the effect of U' is noticeable in both the A- and C-phases. The orbital densities in C-phase attain their saturation values by $U' \simeq 8$. Since we are interested in the region $x \geq 0.5$, we have not plotted orbital densities in A-phase beyond $U' = 8$ – above this value A-phase shifts below $x = 0.5$ at $J_H = 5$ (see Fig.1).

The present calculations produce results that agree with BK and Pai for $U=U'=0$. We are able to recover the G-phase at $x \simeq 1$ and we also obtained the F phase for $J_{AF} \simeq 0$. On inclusion of inter- and intra-orbital interactions, the topology of the phase diagram remains the same. The C-phase grows at the expense of F phase while the G-phase remains unaffected with increasing $\frac{U'}{t}$. This scenario is borne out in the bandwidth controlled experiments of Akimoto et. al.[5] and the schematic phase diagram obtained by Kajimoto et. al[6]. Our results qualitatively agree with the earlier work of Maezono et. al.[19] as well. They included correlations in an MF treatment, but did not get the A-phase close to $x \simeq 0.5$ observed experimentally. Although Fig.15 in Maezono et. al.[20] resembles (with a vanishing A-phase close to $x = 0.5$) our Fig.2, a comparison is quite difficult owing to the very different choice of the parameters (it is also not possible to separate the effects of Coulomb and exchange interactions in their work). In their Monte Carlo treatment, Shen and Ting[22] considered an effective model and obtained a phase diagram. However, the C-phase in the region $0.6 \leq x \leq 0.9$ does not come out of their work. Hotta et. al.[11] have compared exact diagonalization results in one dimension with MF theory and found the agreement to be good. Our MF calculations also suggest that the qualitative trends obtained are in good agreement with the physically expected and experimentally observed results in the manganites.

We note that the value of U' for which the F-phase disappears from the region $x \geq 0.5$ in our calculation is about $\frac{U'}{t} = 12$. Depending on the value of t , corresponding U' is between 1.8 - 3.6 eV. This value is somewhat on the lower side for the range of values available in

literature (the range varies between 3-10 eV)[12, 13, 14]. Although the available values are actually bare values and in phases like F and A, they are bound to go down owing to metallic screening (a treatment of which is beyond the scope of this work) – a problem faced in all theories of correlated systems across a metal-insulator transition. In the foregoing, we have assumed that increase in interactions is qualitatively equivalent to reduction of bandwidth, while in reality, the interactions play more complex roles in addition to charge localization which are not included in our calculation.

In conclusion, we have included orbital correlations in a degenerate double exchange model proposed by Brink and Khomskii for the electron doped, intermediate bandwidth manganites. We observe from a generalized mean-field calculation that the phase diagram captures most of the qualitative features seen experimentally. The orbital orderings obtained are in good agreement with experimental observations. It also agrees with the trends observed across several manganites with changing bandwidths. It would be interesting to include JT coupling and extended range Coulomb terms in the model and observe their effects particularly close to the $x = 0.5$ region.

Acknowledgement

We acknowledge extensive discussions and clarifications at the initial stage with G. V. Pai. We also acknowledge helpful discussions with S. K. Ghatak and R. Pandit. The work is supported by a grant from DST (India). TM acknowledges support from CSIR (India) through a fellowship.

References

- [1] *Physics of Manganites*, edited by T. A. Kaplan and S. D. Mahanty (Kluwer Academic, New York, 1999).
- [2] M. Imada, A. Fujimori and Y. Tokura, Rev. Mod. Phys. **70**, 1039 (1998).
- [3] Y. Tomioka et. al, Phys. Rev. Lett **74**, 5108 (1995).
- [4] H. Kuwahara et. al, Phys. Rev. Lett **82**, 4316 (1999).
- [5] T. Akimoto et. al, Phys. Rev. B **57**, R5594 (1998).
- [6] R. Kajimoto et. al., cond-mat/0110170.
- [7] R. Kajimoto et. al, Phys. Rev. B **60**, 9506 (1999).
- [8] H. Yoshizawa et. al, Phys. Rev. B **58**, R571 (1998).
- [9] J. Brink and D. Khomskii, Phys. Rev. Lett **82**, 1016 (1999).
- [10] K. Kugel and D. Khomskii, Sov. Phys. JETP **37**, 725 (1973).
- [11] T. Hotta, A. Malvezzi and E. Dagotto, Phys. Rev. B **62**, 9432 (2000).
- [12] E. Dagotto, T. Hotta and A. Moreo, Physics Reports, **344**, 1 (2001)..
- [13] J. M. D. Coey et. al, Adv. in Physics **48**, 167 (1999).
- [14] S. Misra, R. Pandit and S. Satpathy, Phys. Rev. B **56**, 2316 (1997); J. Phys. Cond. Matter, **11**, 8561 (1999).
- [15] S. Satpathy et. al, Phys. Rev. Lett. **76**, 960 (1996).
- [16] G. Venkateswara Pai, Phys. Rev. B **63**, 064431 (2001).
- [17] Andrzej M. Oles, Mario Cuoco and N. B. Perkins, cond-mat/0012013.
- [18] The CE phase close to $x \leq 0.5$ appears in some cases in an extremely narrow region for the intermediate bandwidth systems[6, 5, 24]. For $(\text{La}_{0.5}\text{Nd}_{0.5})_{1-x}\text{Sr}_x \text{MnO}_3$, the region of our interest ($z \simeq 0.4$ and $x \geq 0.5$) shows no charge ordering (see Figs. 4 & 5 in[5]).
- [19] R. Maezono, S. Ishihara and N. Nagaosa, Phys. Rev. B. **57**, R13993 (1998).
- [20] R. Maezono, S. Ishihara and N. Nagaosa, Phys. Rev. B. **58**, 11583 (1998).
- [21] The phase identified as canted A-phase by BK is actually a canted G-phase. This phase should be contrasted with the A-phase close to $x = 0.5$ end which is orbitally ordered.

[22] L. Sheng and C. S. Ting, cond-mat/9812374.

[23] In the choice of $J_H S_0$ in eqn.(3), there is an additional factor of 2 in ref.[16].

[24] H. Kawano et. al., Phys. Rev. Lett. **78**, 4253 (1997).

Figure captions

- Fig. 1. Magnetic phase diagram in doping (x) - J_H plane with (a) $U' = 0$ and (b) $U' = 8.0$. All energies are measured in units of t .
- Fig. 2. Magnetic phase diagram in doping (x) - J_{AF} plane with (a) $U' = 0$ and (b) $U' = 8.0$.
- Fig. 3. Canting of the angles θ_{xy} and θ_z in degrees as a function of J_H ($J_{AF}S_0^2 = 0.05$).
- Fig. 4. Orbital densities as a function of doping x for three values of $U' = 0, 4, 8$. The filled symbols are for d_{z^2} and open symbols for $d_{x^2-y^2}$ orbitals. The vertical dotted lines represent the boundary between A- and C-phases for different U' . We choose $J_H S_0 = 5$ here in order to have stable A- and C-phases for a reasonable range of x (see Fig.1) for all three U' values. $J_{AF}S_0^2$ was kept at 0.05.
- Fig. 5. Orbital density versus U' in (a) A-phase at $x = 0.5$ and (b) C-phase at $x = 0.65$. The dotted lines are for d_{z^2} and solid lines are for $d_{x^2-y^2}$ orbitals. $J_H S_0$ and $J_{AF}S_0^2$ were same as in Fig.4.

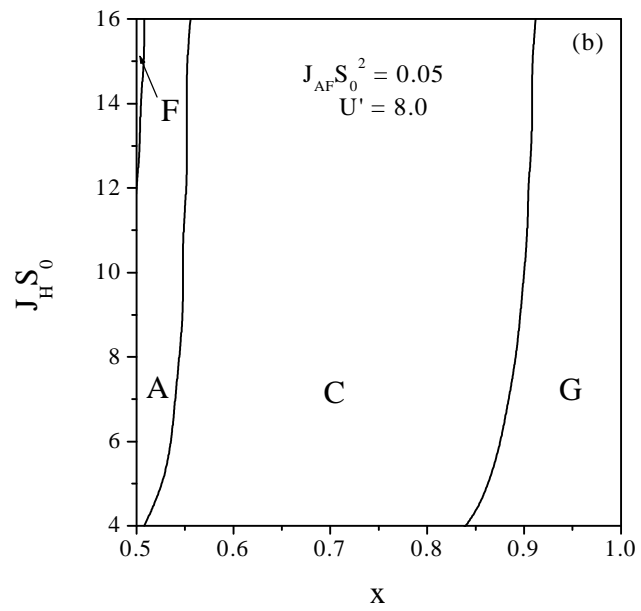
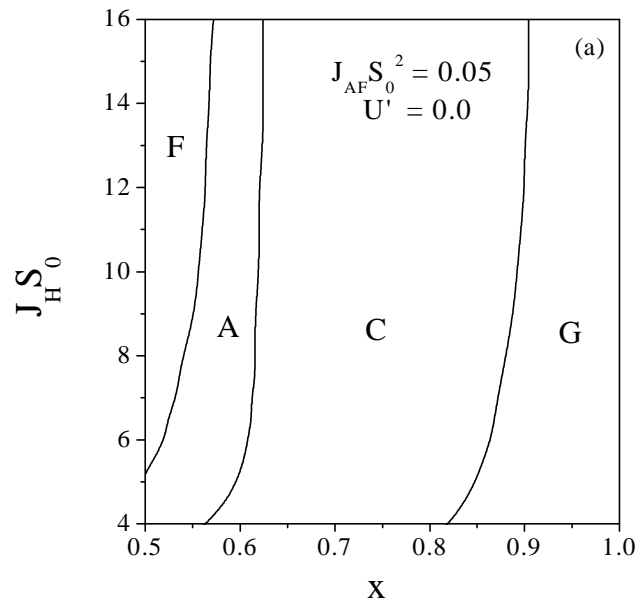


Fig. 1

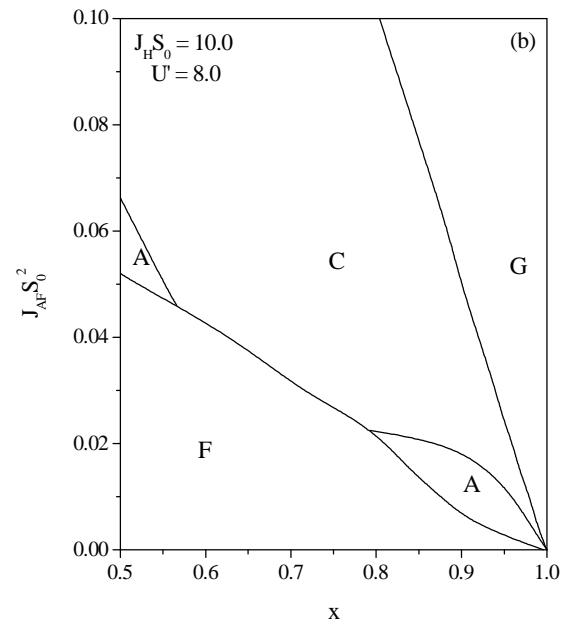
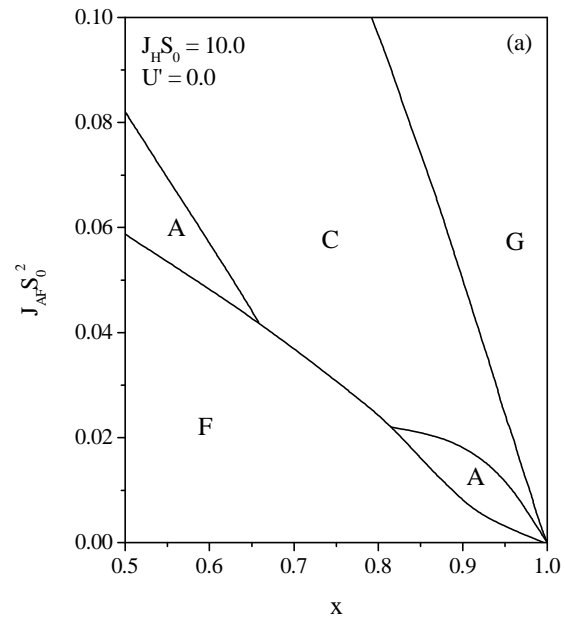


Fig. 2

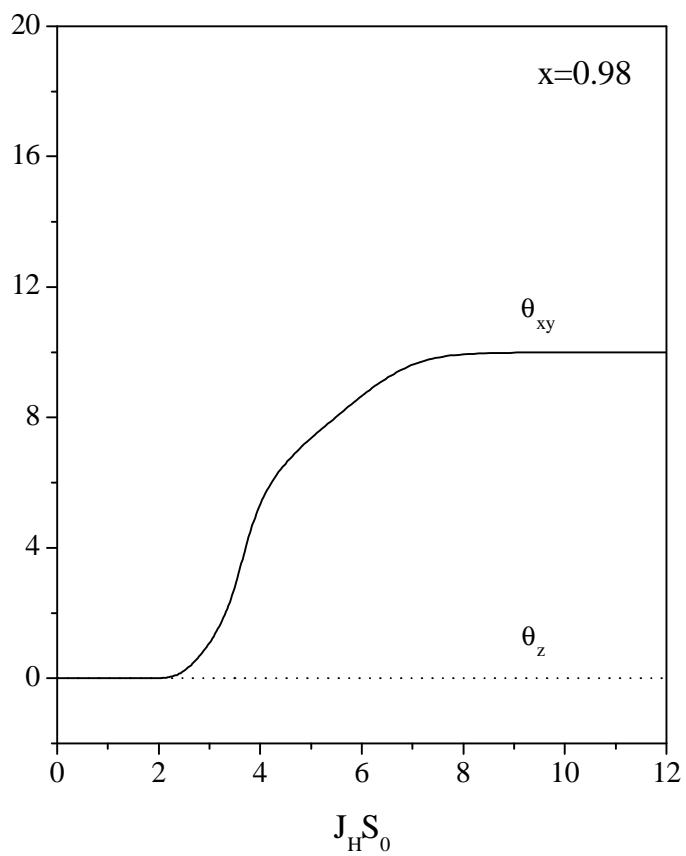


Fig. 3

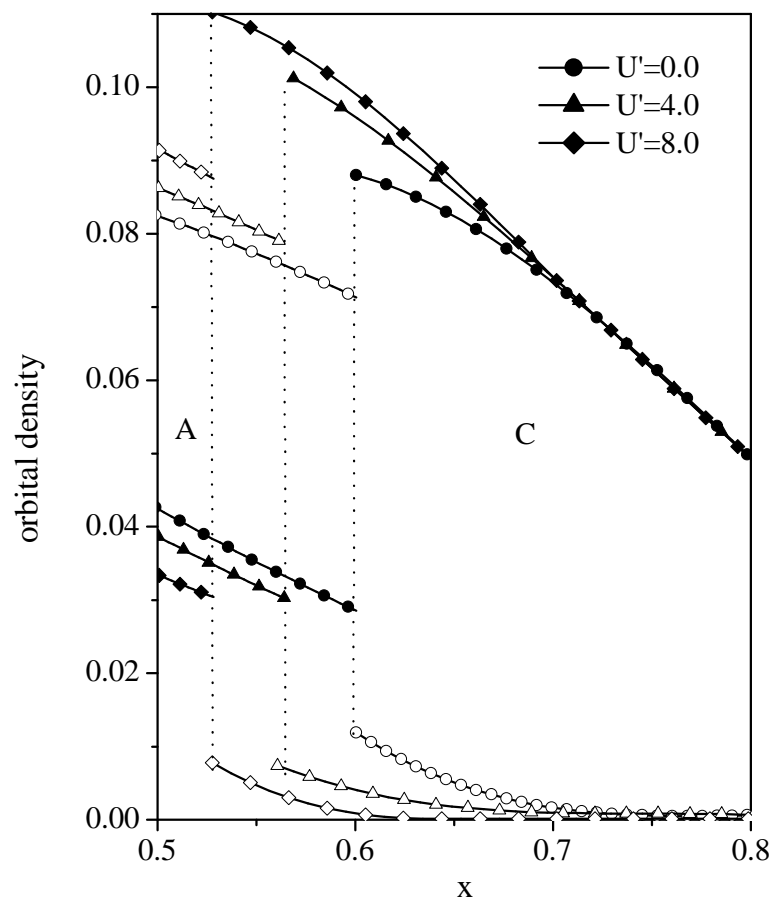


Fig.4

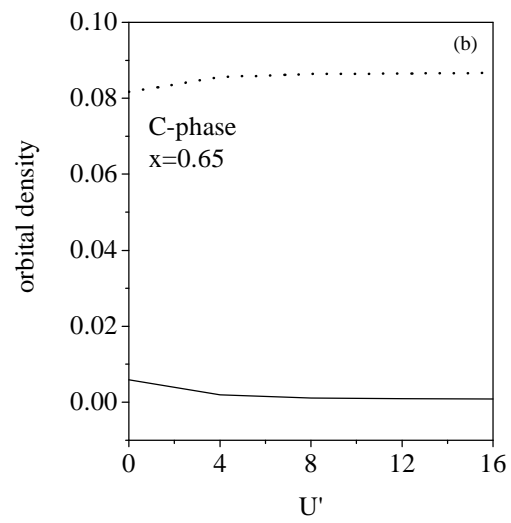
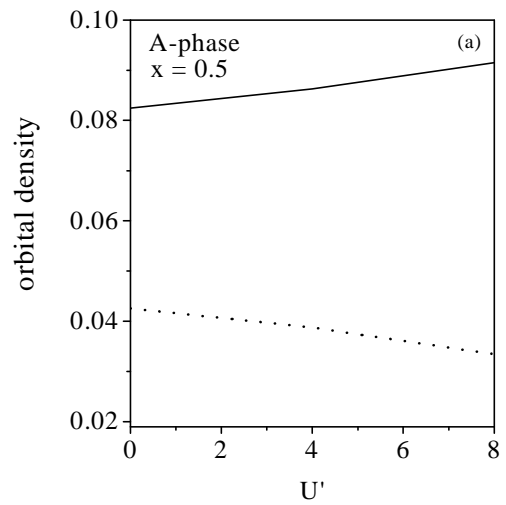


Fig. 5